PHYSICAL REVIEW B **70**, 104520 (2004)

Possible competition between superconductivity and magnetism in $RuSr_2Gd_{1.5}Ce_{0.5}Cu_2O_{10-\delta}$ ruthenocuprate compounds

V. P. S. Awana,* M. A. Ansari, Anurag Gupta, R. B. Saxena, and H. Kishan
National Physical Laboratory, K.S. Krishnan Marg, New Delhi 110012, India

Devendra Buddhikot and S. K. Malik
Tata Institute of Fundamental Research, Homi Bhabha Road, Mumbai 400005, India

(Received 19 January 2004; revised manuscript received 17 May 2004; published 29 September 2004)

The $RuSr_2Gd_{1.5}Ce_{0.5}Cu_2O_{10-\delta}$ (Ru-1222) compounds, with varying oxygen content, crystallize in a tetragonal crystal structure (space group $I4/mmm$). Resistance (R) versus temperature (T) measurements show that the air-annealed samples exhibit superconductivity with superconduting transition temperature (T_c) onset at around 32 K and $R=0$ at 3.5 K. On the other hand, the N_2-annealed sample is semiconducting down to 2 K. Magneto-transport measurements on an air-annealed sample in applied magnetic fields of 3 and 6 T (Tesla) show a decrease in both T_c onset and $T_{R=0}$. Magnetoresistance of up to 20% is observed in the N_2-annealed sample at 2 K and 3 T applied field. The dc magnetization data (M vs T) reveal magnetic transitions (T_{mag}) at 100 K and 106 K, respectively, for both air- and N_2-annealed samples. Ferromagnetic components in the magnetization are observed for both samples at 5 K and 20 K. The superconducting transition temperature (T_c) seems to compete with the magnetic transition temperature (T_{mag}). Our results suggest that the magnetic ordering temperature (T_{mag}) of Ru moments in RuO_6 octahedra may have direct influence/connection with the appearance of superconductivity in Cu-O_2 planes of Ru-1222 compounds.

DOI: 10.1103/PhysRevB.70.104520 PACS number(s): 74.25.Ha, 74.72.Jt, 75.25.+z, 75.30.Cr

I. INTRODUCTION

Recent discovery of the coexistence of magnetism and superconductivity in Ru-1222($RuSr_2(Gd,Ce)_2Cu_2O_{10-\delta}$)[1,2] and Ru-1212($RuSr_2GdCu_2O_{8-\delta}$)[3–6] ruthenocuprates compounds has attracted a great deal of attention. Both Ru-1212 and Ru-1222 compounds are related with the Cu-1212 ($CuBa_2RECu_2O_7$ or RE-123, RE=rare earths) compounds with Ba in the latter replaced by Sr and oxygen deficient CuO_{1-d} chains replaced by RuO_6 octahedra. Further, the oxygen free RE layer between CuO_2 planes in Cu-1212 is replaced by a rocksalt O-(Gd,Ce)-O block in the Ru-1222 structure. Synthesis of both Ru-1212 and Ru-1222 compounds in pure phase has been a problem due to the formation of magnetic $SrRuO_3$ and Gd_2SrRuO_6 in the matrix.[1–6]

By now, it is widely accepted[1,2,4–7] that the Ru moments in RuO_6 octahedra of Ru-1212 and Ru-1222 order magnetically around 100–140 K(T_{mag}), though the exact nature of ordering is still debated.[8–10] Further, superconductivity associated with the CuO_2 planes with transition temperature (T_c) of up to 40 K[1–10] is observed in these compounds. Coexistence of superconductivity and magnetism in these compounds has been indirectly proved by nuclear magnetic resonance (NMR) experiments.[11] At the same time, it is worth mentioning that there exist some reports, which are against the genuine coexistence of superconductivity with magnetism in these compounds.[12,13]

Both the magnetic ordering temperature (T_{mag}) of the Ru moments and the superconductivity (T_c) of the CuO_2 planes are expected to be controlled by the extent of Ru^{4+}/Ru^{5+} ratio in RuO_6 octahedra. The controlling of T_{mag} is due to the mixed Ru^{4+}/Ru^{5+} ratio and that of the T_c is due to the doping of CuO_2 superconducting planes by charge transfer from RuO_6 octahedra. The oxygen content of RuO_6 octahedra or the ratio of Ru^{4+}/Ru^{5+} can be controlled to some extent in Ru-1222, but not in Ru-1212.[14] Therefore, it is of prime interest to vary the oxygen content of RuO_6 octahedra, and study its effect on the T_{mag} and T_c of the Ru-1222 compound. This is the aim of our present work. We have been successful in controlling the T_c of the Ru-1222 compound from 3.5 K to non-superconducting state within the same crystallographic phase. This provided us with an opportunity to compare the T_c and T_{mag} of Ru-1222. Our results indicate that both T_c and T_{mag} compete with each other.

II. EXPERMENTAL DETAILS

The $RuSr_2Gd_{1.5}Ce_{0.5}Cu_2O_{10-\delta}$(Ru-1222) samples were synthesized through a solid-state reaction route from RuO_2, $SrCO_3$, Gd_2O_3, CeO_2, and CuO. Calcinations were carried out on the mixed powder at 1000, 1020, 1040, and 1050 °C each for 24 h with intermediate grindings. The pressed circular pellets were annealed in air for over 48 h at 1050 °C (named "air-annealed"). One of the air-annealed pellets was further annealed in nitrogen gas (1 atm) at 420 °C for 24 h and subsequently cooled slowly to room temperature (named "N_2-annealed"). X-ray diffraction (XRD) patterns were obtained at room temperature [MAC Science: MXP18VAHF; CuK_α radiation]. Magnetization measurements were performed on a SQUID magnetometer (Quantum Design: MPMS-5S). Resistivity measurements under applied magnetic fields of up to 9 T were made in the temperature range of 2–300 K using a four-point-probe technique (PPMS, Quantum Design).

1098-0121/2004/70(10)/104520(6)/$22.50

©2004 The American Physical Society

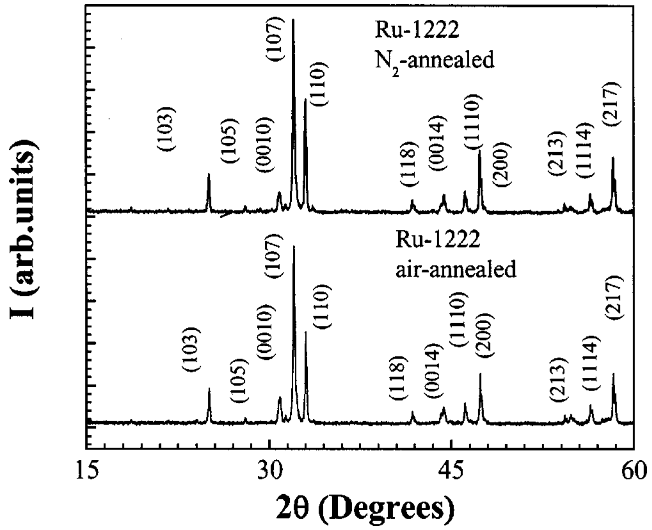

FIG. 1. Observed x-ray diffraction pattern for the air- and N_2-annealed $RuSr_2Gd_{1.5}Ce_{0.5}Cu_2O_{10-\delta}$ samples.

III. RESULTS AND DISCUSSION

A. X-ray diffraction and phase formation

Both air- and N_2 annealed Ru-1222 compounds crystallize in a tetragonal structure (space group $I4/mmm$) with $a=b=3.8427(7)$ Å and $c=28.4126(8)$ Å for the former and $a=b=3.8498(3)$ Å and $c=28.4926(9)$ Å for the latter. The increase in the lattice parameters of the N_2-annealed sample indicates an overall decrease in oxygen content of the sample. X-ray diffraction patterns for both the air- and N_2-annealed samples are shown in Fig. 1. Small impurity peaks (marked with "*") are seen close to the background. The presence of small amounts of $SrRuO_3$ and/or $GdSr_2RuO_6$ in Ru-1222 samples has been noted earlier also.[1,2,5] Our currently studied samples are, in fact, far better in terms of their phase purity, compared to those reported earlier by various authors. As mentioned earlier, Ru-1222 is structurally related to the Cu-1212, e.g., $CuBa_2YCu_2O_{7-\delta}$ phase with Cu in the charge reservoir in the latter replaced by Ru such that the Cu-O chain is replaced by a RuO_2 sheet. Furthermore, a three-layer fluorite-type block, instead of a single oxygen-free R (R= rare earth element) layer, is inserted between the two CuO_2 planes of the Cu-1212 structure[15] to get the Ru-1222 phase.

B. Electrical transport under magnetic field and magnetism

The resistance versus temperature (R-T) behavior of air-annealed Ru-1222 sample in magnetic fields of 0 T, 3 T, and 6 T in the temperature range of 2–300 K is shown in Fig. 2. The resistance of the compound increases with decrease in temperature indicating its semiconducting behavior. However, in zero applied field, the compound shows a sharp drop in its resistance at around 35 K (T_c^{onset}) with zero resistance state occurring at 3.5 K $T_c^{(R=0)}$. Rather broad superconducting transition and the low value of T_c (3.5 K) point towards low carrier concentration in the air-annealed sample. It is well known that superconducting properties of Ru-1222 can be considerably improved by annealing in oxygen under pressure.[10,16] In fact, by annealing in 100-atm-O_2, one can achieve T_c of up to 40–45 K.[10] By normal pressure (1 atm) O_2 annealing, the T_c of the air-annealed sample could not be increased significantly.

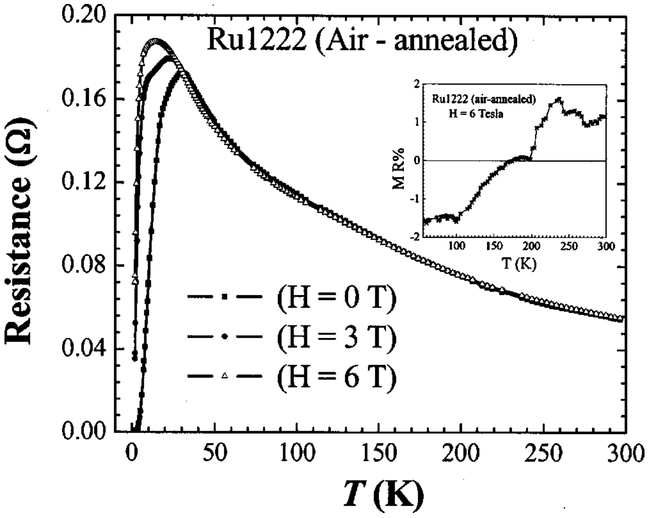

FIG. 2. Resistance (R) vs temperature (T) plots in 0, 3, and 6 T applied magnetic fields for air-annealed $RuSr_2Gd_{1.5}Ce_{0.5}Cu_2O_{10-\delta}$ sample. Inset shows the magnetoresistance (MR%) vs T plot for 6 T applied field.

In applied magnetic fields of 3 and 6 T, though the normal state (above T_c onset) resistance behavior of Ru-1222 is essentially the same as in zero field, both T_c^{onset} and $T_c^{(R=0)}$ decrease with applied field. For example, T_c^{onset} is 32 K, 27 K, and 15 K, respectively, for 0, 3, and 6 T applied fields and $T_c^{(R=0)}$ state is not observed under these applied magnetic fields. Magnetoresistance (MR) defined as

$$\mathrm{MR}\,\% = [(R_H - R_0)/R_H] \times 100 \tag{1}$$

is plotted in inset of Fig. 2. Though the observed MR% is small, it changes sign at around 180 K being positive above 180 K and negative below 180 K. The sign change of MR at 180 K might be related to the magnetic structure transformation at the said temperature. We shall discuss this later after presenting magnetization results.

Figure 3 depicts the resistance versus temperature (R-T) behavior for the N_2-annealed Ru-1222 sample in magnetic fields of 0, 3, and 6 T. The R-T behavior of this compound is semiconducting down to 2 K. No superconducting transition is observed in the whole temperature range studied (2–300 K). Further, in the low temperature region, an appreciable MR is seen in this sample. Magnetoresistance, as a function of applied field, at temperatures of 5 and 10 K, is plotted in the inset of Fig. 3. MR of >20% is observed at 5 K in an applied field of up to 9 T. At 2 K, around 20% MR is seen even in low applied field of 3 T (plot not shown).

Figure 4 shows the magnetic susceptibility (χ) vs temperature (T) behavior in the temperature range of 2–300 K for an air-annealed Ru-1222 sample in an applied field of 100 Oe, measured in both zero-field-cooled (ZFC) and field-cooled (FC) modes. The χ vs T plot shows the branching of

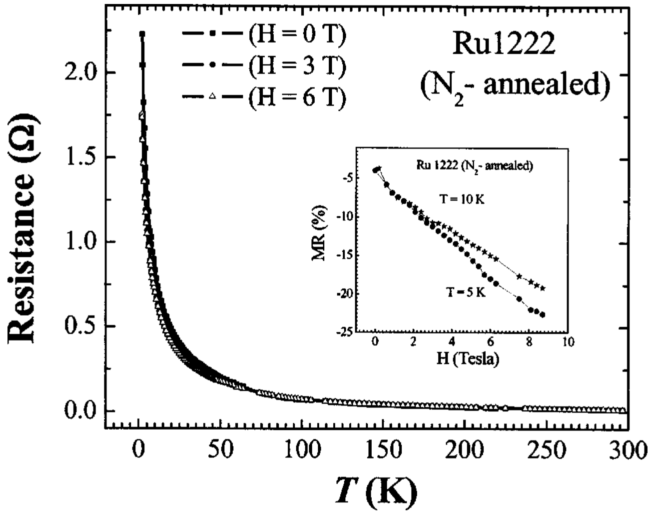

FIG. 3. Resistance (R) vs temperature (T) plots in 0, 3, and 6 T applied magnetic fields for N_2-annealed $RuSr_2Gd_{1.5}Ce_{0.5}Cu_2O_{10-\delta}$ sample. Inset shows the magnetoresistance (MR%) at 5 K in applied fields up to 9 T.

ZFC and FC curves at around 95 K and the magnetic susceptibility starts shooting up at around 100 K (T_{mag}). In fact, the susceptibility of the Ru-1222 compound starts deviating from normal Curie-Weiss paramagnetic behavior at around 165–200 K. It has been reported that the Ru moments in Ru-1222 order antiferromagnetically at around 180 K, which later develops into a canted ferromagnetism at lower temperatures (T_{mag}).[1,2,6] As mentioned earlier, the exact nature of magnetic ordering in low temperature region is still debated. The 180 K paramagnetic to antiferromagnetic transition could be seen in magneto-transport measurements also, where small positive MR changes to negative MR below this temperature (inset, Fig. 2).

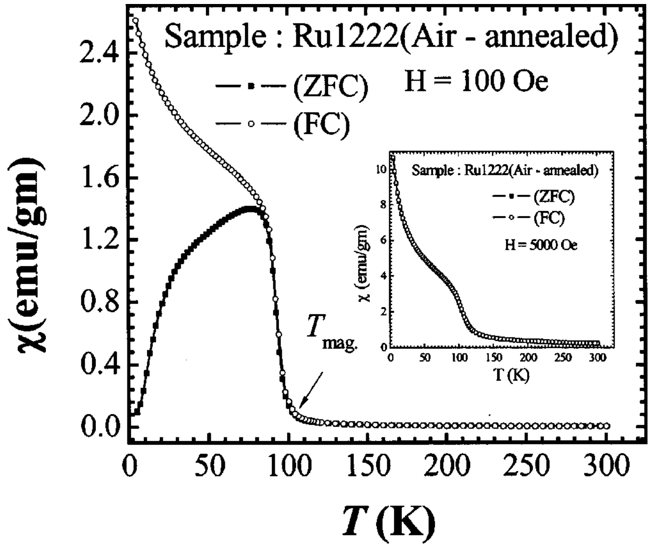

FIG. 4. Magnetic susceptibility (χ) vs temperature (T) plot for air-annealed $RuSr_2Gd_{1.5}Ce_{0.5}Cu_2O_{10-\delta}$ in both ZFC and FC modes with applied field of 100 Oe, inset shows the same for H =5000 Oe.

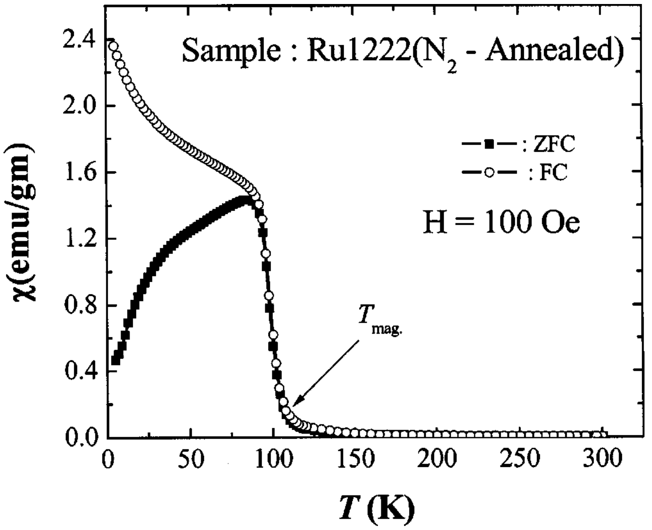

FIG. 5. Magnetic susceptibility (χ) vs temperature (T) plot for N_2-annealed $RuSr_2Gd_{1.5}Ce_{0.5}Cu_2O_{10-\delta}$ in both ZFC and FC modes with applied field of 100 Oe.

The characteristic temperature T_{mag} is weakly dependent on an applied magnetic field $H < 100$ Oe. For $H > 1000$ Oe, both ZFC and FC magnetization curves are merged with each other (see inset, Fig. 4). In fact, no ZFC-FC branching is observed down to 2 K in the 5000 Oe field. This is in general agreement with earlier reports.[1,2] Superconductivity is not seen in terms of diamagnetic transition (T_d) in an applied field of $H = 100$ Oe (Fig. 4). It is known that, due to internal magnetic fields, these compounds are in a spontaneous vortex phase (SVP) even in zero external field.[17] For $T_d < T < T_c$, the compound remains in a mixed state. Hence though $R = 0$ is achieved at relatively higher temperatures (3.5 K, see Fig. 2), the diamagnetic response is seen at much lower temperatures and that too in quite small applied magnetic ($H_{c1} < 25$ Oe) fields. Hence, we could conclude that the magnetic susceptibility (χ) vs T behavior shown in Fig. 4 does not exclude the presence of superconductivity in the presently studied air-annealed Ru-1222 sample. At lower applied field of 5 Oe, the compound exhibits a diamagnetic transition (T_d) below the $T_c^{(R=0)}$ state (curve not shown).

The χ-T behavior in the temperature range of 2–300 K for the N_2-annealed Ru-1222 sample in an applied field of 100 Oe, measured in both zero-field-cooled (ZFC) and field-cooled (FC) modes, is shown in Fig. 5. The general shape of FC and ZFC magnetization plots is similar to that for air-annealed sample. The interesting change is that T_{mag} (defined earlier) has increased to 106 K for the N_2-annealed sample. It is worth mentioning that the N_2-annealed sample is not superconducting down to 2 K (Fig. 3, R vs T results).

C. Ferromagnetic component

Magnetization (M) vs applied field (H) isotherm at 5 K for the air-annealed Ru-1222 sample is shown in Fig. 6. The magnetization starts saturating above 6 T field in both directions. The M-H plot is further zoomed in applied field of −900 Oe to 900 Oe, and shown in the inset of Fig. 6. At 5 K,

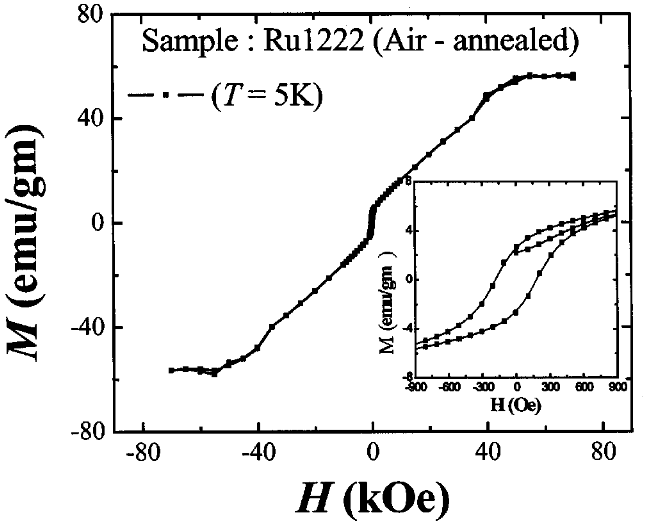

FIG. 6. Magnetization-field (*M-H*) hysteresis loop for air-annealed $RuSr_2Gd_{1.5}Ce_{0.5}Cu_2O_{10-\delta}$ at 5 K. Inset shows the same for $-900\ \text{Oe} \leqslant H \leqslant +900\ \text{Oe}$.

the returning moment (M_{rem}) i.e., the value of magnetization at zero returning field and the coercive field (H_c), i.e., the value of applied returning field needed to get zero magnetization, are, respectively, 2.50 emu/g and 160 Oe (inset Fig. 6). It is known that the Gd (magnetic rare earth) in this compound orders magnetically below 2 K and Ce remains in a tetravalent, nonmagnetic state, hence the M_{rem} and H_c arising from the ferromagnetic hysteresis loops do belong to Ru only. Interestingly, for Ru-1222, the hysteresis loops are reported to be quite narrow.[4,5] This indicates that, in Ru-1222, the ferromagnetic domains are less anisotropic and more rigid. The *M-H* loop at 20 K for the air-annealed Ru-1222 sample is shown in Fig. 7, which shows a decreased M_{rem}(1 emu/g) and H_c(75 Oe) compared to the 5 K plot in Fig. 6. The values of both M_{rem} and H_c decrease with *T*.

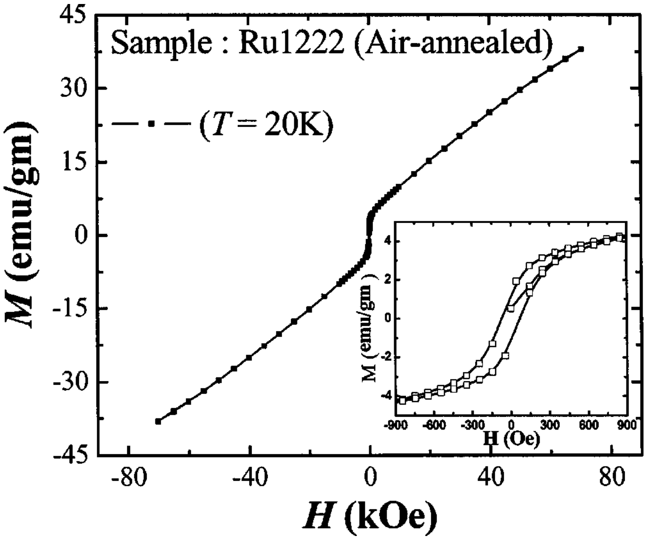

FIG. 7. Magnetization-field (*M-H*) hysteresis loop for air-annealed $RuSr_2Gd_{1.5}Ce_{0.5}Cu_2O_{10-\delta}$ at 20 K. Inset shows the same for $-900\ \text{Oe} \leqslant H \leqslant +900\ \text{Oe}$.

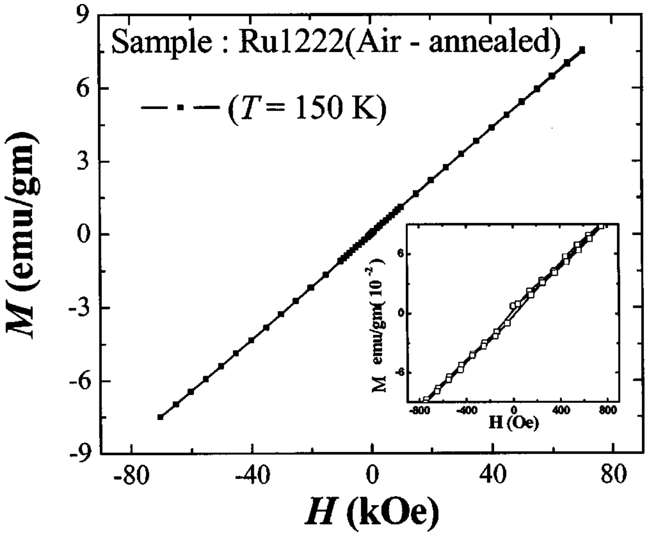

FIG. 8. Magnetization-field (*M-H*) hysteresis loop for air-annealed $RuSr_2Gd_{1.5}Ce_{0.5}Cu_2O_{10-\delta}$ sample at 150. Inset shows the same for $-900\ \text{Oe} \leqslant H \leqslant +900\ \text{Oe}$.

Hysteresis loops were not seen at higher temperatures above T_{mag}. For example, the *M-H* plot at 150 K is seen as completely linear with field (Fig. 8), and no hysteresis loops were visible even after zooming at low fields (inset of Fig. 8).

Figure 9 depicts the *M-H* plot at 5 K for the N_2-annealed Ru-1222 sample. This plot is similar to that observed for the air-annealed Ru-1222 sample. The zoomed ferromagnetic component is shown in the inset. The interesting difference, when compared with air-annealed sample, is that *M* does not saturate in applied fields up to 7 T. This is in contrast to the *M-H* plot for the air-annealed sample at 5 K for which *M* saturates in a field of 6 T (see Fig. 6). The *M-H* plot for N_2-annealed sample is further zoomed in applied field of −900 Oe to 900 Oe, and shown in the inset of Fig. 9. A ferromagnetic loop is seen clearly with M_{rem} (2 emu/g) and

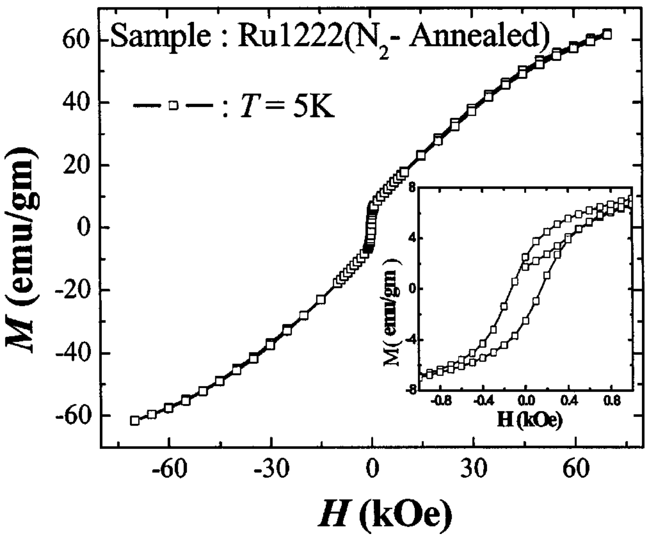

FIG. 9. Magnetization-field (*M-H*) hysteresis loop for N_2-annealed $RuSr_2Gd_{1.5}Ce_{0.5}Cu_2O_{10-\delta}$ sample at 5 K. Inset shows the same for $-900\ \text{Oe} \leqslant H \leqslant +900\ \text{Oe}$.

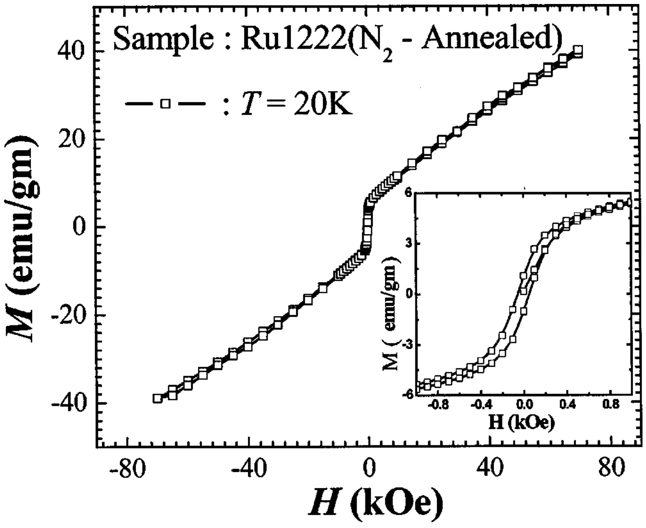

FIG. 10. Magnetization-field (*M*-*H*) hysteresis loop for N_2-annealed $RuSr_2Gd_{1.5}Ce_{0.5}Cu_2O_{10-\delta}$ sample at 20 K. Inset shows the same for $-900\ Oe \leqslant H \leqslant +900$ Oe.

H_c (170 Oe). The *M*-*H* loop at 20 K for the N_2-annealed sample is shown in Fig. 10, which reveals decreased M_{rem} (1 emu/g) and H_c(70 Oe). The trend of M_{rem} and H_c for the N_2-annealed sample is similar to that of an air-annealed sample, i.e., both decrease with increase in temperature. The *M*-*H* loops were not seen above T_{mag} for the N_2-annealed samples also.

The results presented above for both air- and N_2-annealed presently studied Ru-1222 samples may be summarized as follows:

(1) Both air- and N_2-annealed samples crystallize in a single-phase tetragonal structure (space group $I4/mmm$).

(2) The air-annealed sample is superconducting with $T_c^{(R=0)}$ of 3.5 K, while the N_2-annealed is not superconducting down to 2 K. The N_2-annealed sample exhibits negative magnetoresistance of up to 20% at 5 K.

(3) Both air- and N_2 -annealed samples order magnetically, with T_{mag} of nearly 100 K for the former and 106 K for the latter.

(4) Both air- and N_2-annealed samples exhibit ferromagnetic loops below T_{mag}. The relative width of loops is more (higher M_{rem} and H_c) for the air-annealed sample compared to that of the N_2-annealed sample at a fixed temperature.

(5) For the air-annealed sample, the *M*-*H* behavior at 5 K exhibits near saturation above 6 T. However, for the N_2 annealed sample, *M* is not saturated up to an applied field of 7 T.

We now discuss these results point by point. As far as the phase formation and crystallization of the two Ru-1222 samples is concerned, it seems that there is some scope for oxygen to get released from RuO_6 octahedra while still maintaining its crystal structure. In fact, another school of thought also exists, which believes in the release of oxygen from rocksalt O-(Gd,Ce)-O block and not from RuO_6 in Ru-1222. Recent spectroscopic studies on Ru-1222 do show indications towards valence fluctuations of Ru^{4+}/Ru^{5+} and hence some variation in oxygen content of RuO_6 octahedra.[18] It has been reported earlier that the oxygen content of Ru-1222 is tunable to some extent by N_2/Ar annealing but not for Ru-1212.[14] Thus it has been possible for us, in the present study, to get both air- and N_2-annealed Ru-1222 samples in the same crystal structure. Decreased oxygen content of the N_2-annealed sample is indicated by increased c-parameter of the sample (the exact oxygen content has not been determined).

As far as the second point is concerned, the air-annealed sample is superconducting but the N_2-annealed sample is not. Further, the normal state conduction, though semiconducting for both samples, is relatively better for the air-annealed sample. This indicates that the air-annealed sample has relatively more mobile hole-carriers than the N_2-annealed sample. The doping for mobile holes in widely believed conducting/superconducting $Cu\text{-}O_2$ planes in RE-123 compounds takes place by charge transfer from oxygen variable redox $CuO_{1-\delta}$ chains. In Ru−1222, the role of the redox layer is supposedly played by RuO_6 octahedra. In the N_2-annealed sample, the Ru^{4+}/Ru^{5+} ratio will be different than that in an air-annealed sample, and hence the number of transferred mobile holes to $Cu\text{-}O_2$ planes will be different. As far as magneto-transport is concerned, no appreciable MR is seen above T_{mag} for both samples. For the air-annealed superconducting sample, the broadening of transition under field is seen and is similar to that in other HTSC compounds. For the N_2-annealed sample, negative MR of around 20% is seen at 2 K. As we know from present magnetization measurements and various other earlier reports, that the low temperature magnetism of Ru-1222 is complex and calls for magnetic phase separation including spin glass,[10] canted antiferromagnetism,[19] or both simultaneously. Though the magnetic structure of Ru-1222 is not yet revealed by low temperature neutron scattering measurements, one thing is apparent that the compound possesses complex low temperature magnetism. In such situations, appreciable MR is expected due to tunnelling between various magnetic domains arising from the magnetically phase separated system. The N_2-annealed sample is highly underdoped and hence one presumes that electrical transport conduction is mainly through the RuO_6 layer, where magnetic scattering does take place. The role of magnetic charge spin scattering has earlier been observed in Ru-1212, where T_{mag} is clearly seen as a hump in resistivity measurements.[4,12] To our knowledge, this is the first observation of finding appreciable negative MR at 2 K in a non-superconducting Ru-1222 compound. This is in conformity with the earlier reports of magnetic phase separation at low temperature in Ru-1222.[10,19]

The third point is comprised of the fact that, for superconducting air-annealed sample, T_{mag} is 100 K while the same is 106 K for nonsuperconducting N_2-annealed sample. As the T_c (superconducting transition temperature) increases, the T_{mag} (magnetic transition temperature of Ru) decreases. This is further demonstrated by the fact that 100-atm-O_2 postannealed sample possesses T_c of 43 K along with T_{mag} of around 90 K.[21] T_{mag} depends weakly on the measuring dc magnetic field. Hence one should be careful in comparing the T_{mag} and T_c of various Ru-1222 samples. Also, one should be reminded of the fact that the decreased number of mobile carriers in Cu-O_2 planes of the N_2-annealed sample along with other structural parameters may also be partly responsible for the nonsuperconducting behavior. One cannot explicitly say that increased T_{mag} is responsible for the decreased superconductivity of the system. What is apparent though, is the possible competing nature of T_{mag} and T_c.

As discussed in point (1) above, the Ru^{4+}/Ru^{5+} ratio in variously processed Ru-1222 samples is supposed to be different. The amount of Ru^{4+} will be higher in the N_2-annealed sample.[14,18] T_{mag} originates from the ordering of Ru moments in RuO_6 octahedra. Changed amounts of Ru^{4+}/Ru^{5+} magnetic spin contribution is responsible for different T_{mag} of the two compounds. A higher content of Ru^{4+} gives rise to increased T_{mag}.

The fourth point says that though both compounds have ferromagnetic domains at low temperatures below T_{mag}, the characteristic values of M_{rem} and H_c are relatively higher for the air-annealed sample. Our detailed microstructural studies earlier for Ru-1222 showed that the observed superlattice structures due to tilt of RuO_6 octahedra[20] might be coupled with the weak ferromagnetic domains constructed by ordering of the canted Ru moments below the magnetic transition temperature (T_{mag}). Hence coupling of ferromagnetic domains depends on the long-range ordering of tilted RuO_6 octahedras in a given Ru-1222 system. In the N_2-annealed sample, the long-range superstructures may break down relatively at smaller length scale than in an air-annealed sample due to less oxygen in RuO_6 octahedra of the same giving rise to weak coupling of the ferromagnetic domains. This will give rise to lower values of M_{rem} and H_c. This also explains the fifth point regarding the observed saturation of the *M-H* curve for the air-annealed sample and not for the N_2-annealed sample. The saturation of *M-H* is dependent on the long range coupling of aligned ferromagnetic domains, which is observed for the air-annealed sample only. Long range coupling of aligned moments is directly dependent on the stability of RuO_6 octahedra tilt angle superstructures, which is certainly less for the N_2-annealed sample due to break down in the homogenous oxygen content close to 6.0 in the octahedra. In earlier reports also, the *M-H* plots at 5 K for superconducting Ru-1222 samples, saturated below an applied field of 7 T.[1,2,16,21]

IV. SUMMARY AND CONCLUSIONS

The Ru-1222 ruthenocuprate compounds have been synthesized with both magneto-superconducting (air-annealed) and only magnetic (N_2-annealed) properties. The same crystal structure is maintained for both compounds. The Ru magnetic ordering temperature (T_{mag}) is higher for the nonsuperconducting sample than for the superconducting sample. M-H plots at 5 K saturate below 6 T applied field for the superconducting sample, but not for the nonsuperconducting sample. These results could be explained on the basis of the presence of mixed valency of Ru^{4+}/Ru^{5+} in these compounds. It is apparent that magnetic order of Ru in RuO_6 octahedra and superconductivity (T_c) in Cu-O_2 planes are intimately related with each other, indicating the coexistence of magnetism and superconductivity in Ru-1222 compounds.

ACKNOWLEDGMENT

Authors from NPL thank Professor Vikram Kumar (DNPL) for his encouragement and keen interest in the present work.

---

*Author to whom correspondence should be addressed. Email address: awana@mail.nplindia.ernet.in

[1] I. Felner, U. Asaf, Y. Levi, and O. Millo, Phys. Rev. B **55**, R3374 (1997).

[2] I. Felner and U. Asaf, Int. J. Mod. Phys. B **12**, 3220 (1998).

[3] L. Bauernfeind, W. Widder, and H. F. Braun, Physica C **254**, 151 (1995).

[4] C. Bernhard, J. L. Tallon, Ch. Niedermayer, Th. Blasius, A. Golnik, E. Brücher, R. K. Kremer, D. R. Noakes, C. E. Stronack, and E. J. Asnaldo, Phys. Rev. B **59**, 14 099 (1999).

[5] J. L. Tallon, J. W. Loram, G. V. M. Williams, and C. Bernhard, Phys. Rev. B **61**, R6471 (2000).

[6] V. P. S. Awana, S. Ichihara, J. Nakamura, M. Karppinen, and H. Yamauchi, Physica C **378–381**, 249 (2002).

[7] A. Butera, A. Fainstein, E. Winkler, and J. Tallon, Phys. Rev. B **63**, 054442 (2001).

[8] J. W. Lynn, B. Keimer, C. Ulrich, C. Bernhard, and J. L. Tallon, Phys. Rev. B **61**, R14 964 (2000).

[9] V. P. S. Awana, T. Kawashima, and E. Takayama-Muromachi, Phys. Rev. B **67**, 172502 (2003).

[10] C. A. Cardoso, F. M. Araujo-Moreira, V. P. S. Awana, E. Takayama-Muromachi, O. F. de Lima, H. Yamauchi, and M. Karppinen, Phys. Rev. B **67**, 020407(R) (2003).

[11] Y. Tokunaga, H. Kotegawa, K. Ishida, Y. Kitaoka, H. Takigawa, and J. Akimitsu, Phys. Rev. Lett. **86**, 5767 (2001).

[12] V. P. S. Awana, S. Ichihara, J. Nakamura, M. Karppinen, H. Yamauchi, Jinbo Yang, W. B. Yelon, W. J. James, and S. K. Malik, J. Appl. Phys. **91**, 8501 (2002).

[13] C. W. Chu, Y. Y. Xue, S. Tsui, J. Cmaidalka, A. K. Heilman, B. Lorenz, and R. L. Meng, Physica C **335**, 231 (2000).

[14] M. Matvejeff, V. P. S. Awana, H. Yamauchi, and M. Karppinen, Physica C **392–396**, 87 (2003).

[15] N. Sakai, T. Maeda, H. Yamauchi, and S. Tanaka, Physica C **212**, 75 (1993).

[16] M. T. Escote, V. A. Meza, R. F. Jardim, L. Ben-Dor, M. S. Torikachvill, and A. H. Lacerda, Phys. Rev. B **66**, 144503 (2002).

[17] E. B. Sonin and I. Felner, Phys. Rev. B **57**, R14 000 (1998).

[18] V. P. S. Awana, M. Karppinen, H. Yamauchi, R. S. Liu, J. M. Chen, and L.-Y. Jang, J. Low Temp. Phys. **131**, 1211 (2003).

[19] I. Živkovic, Y. Hirai, B. H. Frazer, M. Prester, D. Drobac, D. Ariosa, H. Berger, D. Pavuna, G. Margaritondo, I. Felner, and M. Onellion, Phys. Rev. B **65**, 144420 (2002).

[20] Tadahiro Yokosawa, Veer Pal Singh Awana, Koji Kimoto, Eiji Takayama-Muromachi, Maarit Karppinen, Hisao Yamauchi, and Yoshio Matsui, Ultramicroscopy **98**, 283 (2004).

[21] V. P. S. Awana, E. Takayama-Muromachi, M. Karppinen, and H. Yamauchi, Physica C **390**, 233 (2003).